molecules

MDPI

Article

Effects of $LiBF_4$ Addition on the Lithium-Ion Conductivity of $LiBH_4$

Laura M. de Kort [1], Valerio Gulino [1], Didier Blanchard [2] and Peter Ngene [1,*]

[1] Materials Chemistry and Catalysis, Department of Chemistry, Debye Institute for Nanomaterials Science, Utrecht University, Universiteitsweg 99, 3584 CS Utrecht, The Netherlands; l.m.dekort@uu.nl (L.M.d.K.); v.gulino@uu.nl (V.G.)

[2] The European Synchrotron Facility (ESRF), 71 Avenue des Martyrs, 38000 Grenoble, France; didier.blanchard@esrf.fr

* Correspondence: p.ngene@uu.nl

Abstract: Complex hydrides, such as $LiBH_4$, are a promising class of ion conductors for all-solid-state batteries, but their application is constrained by low ion mobility at room temperature. Mixing with halides or complex hydride anions, i.e., other complex hydrides, is an effective approach to improving the ionic conductivity. In the present study, we report on the reaction of $LiBH_4$ with $LiBF_4$, resulting in the formation of conductive composites consisting of $LiBH_4$, LiF and lithium *closo*-borates. It is believed that the in-situ formation of *closo*-borate related species gives rise to highly conductive interfaces in the decomposed $LiBH_4$ matrix. As a result, the ionic conductivity is improved by orders of magnitude with respect to the Li-ion conductivity of the $LiBH_4$, up to 0.9×10^{-5} S cm^{-1} at 30 °C. The insights gained in this work show that the incorporation of a second compound is a versatile method to improve the ionic conductivity of complex metal hydrides, opening novel synthesis pathways not limited to conventional substituents.

Keywords: solid-state electrolytes; complex hydrides; lithium borohydride; ionic conductivity; ion substitution; interface effects

check for updates

Citation: de Kort, L.M.; Gulino, V.; Blanchard, D.; Ngene, P. Effects of $LiBF_4$ Addition on the Lithium-Ion Conductivity of $LiBH_4$. *Molecules* **2022**, *27*, 2187. https://doi.org/10.3390/molecules27072187

Academic Editor: Ewa C. E. Rönnebro

Received: 2 February 2022
Accepted: 22 March 2022
Published: 28 March 2022

1. Introduction

In our current society, rechargeable lithium-ion batteries are crucial energy storage devices for a wide variety of applications, ranging from small portable electronics to electric vehicles. The performance and safety requirements for automotive electrification and grid-energy storage systems, however, cannot be met by the commercially available batteries [1,2]. Hence, the development of batteries with higher energy densities and improved safety is crucial. The performance limitations in commercial Li-ion batteries are caused by their organic liquid electrolytes that often suffer from poor electrochemical and thermal stability, which poses safety risks and limits storage capacity [3]. Replacement of the liquid electrolyte with a solid electrolyte could overcome these persistent problems. Solid-state electrolytes (SSEs) are inherently safer and, in many cases, compatible with high energy density electrodes, such as metallic lithium [4]. Consequently, the realization of all-solid-state batteries implementing SSEs can lead to safer batteries that store more energy.

The anticipated benefits of SSEs has led to a growing number of studies on inorganic lithium ion conductors [5], such as garnet-type [6,7], perovskite-type [8,9] and sulphide-type materials [10,11] The research scope on potential Li-ion conductors was recently extended to complex metal hydrides following the surprising discovery of fast Li-ion mobility in $LiBH_4$ [12]. Complex metal hydrides exhibit several unique material properties that are interesting for battery application, i.e., low molecular weight, easy deformability and high compressibility, and compatibility with a lithium metal anode [13–16]. Among others, these benefits have spurred research on complex metal hydrides as promising SSEs for all-solid-state Li-ion batteries.

A main disadvantage for metal hydrides, and many other solid electrolytes, is their low room temperature (RT) ionic conductivity. Complex hydrides typically exhibit high ionic conductivity as a result of a reversible structural phase change that requires high temperatures [12,17,18]. For example, fast lithium-ion mobility and high conductivity (~10^{-3} S cm^{-1}) in $LiBH_4$ is only observed after a phase transition from the orthorhombic to the hexagonal phase at 110 °C [12]. Therefore, the development of strategies that enhance RT Li-ion conductivity is of major importance for the application of metal hydride-based ion conductors.

From various methods developed to boost ionic conductivity in complex hydrides, e.g., nanoconfinement and interface engineering [19–22], partial ionic substitution has proven to be particularly useful [23–28]. Previous reports reveal that the incorporation of lithium halides (LiX, with X = Br^-, I^-) or lithium amide ($LiNH_2$) in the $LiBH_4$ crystal structure leads to significant improvement in ionic transport. Depending on the substituting anion, partial anionic substitution of BH_4^- either leads to stabilization of the conductive hexagonal phase at lower temperatures (*h*-$Li(BH_4)_{1-y}(X)_y$) [15,29,30] or to the formation of a new highly conductive crystal structure, e.g., $Li_2(BH_4)(NH_2)$ [27,28].

The use of anion substitution for conductivity enhancement in $LiBH_4$ has so far been limited to the addition of halides and other complex hydrides. A complex anion that could also be interesting as a partial substituent for $[BH_4]^-$ is the $[BF_4]^-$ anion. $LiBF_4$ is a well-known Li-ion conductor for liquid electrolytes, but it has not been investigated as SSE because it exhibits very poor conductivity as a solid electrolyte. Partial ionic substitution of BF_4^- in $LiBH_4$ has been investigated as a method to improve the hydrogen storage properties of metal borohydrides [31–35]. Different from LiX and $LiNH_2$, in this case, it was reported that F^- is exchanged for H^-, forming a $[BH_{4-x}F_x]^-$ complex. Theoretical studies proposed that intramolecular hydrogen-fluorine exchange in MBH_4-MBF_4 systems (M = Li, Na, K) significantly alters the borohydride structure [31–33]. It has been speculated that the strong electronegativity of the fluoride atom weakens the force of attraction between the B and the H in the complex anion [36]. Similarly, electrostatic interactions between the $[BH_{4-x}F_x]^-$ anion with the Li^+ cation could be attenuated, thereby improving Li-ion mobility. The predicted effects in the $LiBH_4$-$LiBF_4$ system for hydrogen storage have been experimentally reported by Richter et al. [36]. However, it was demonstrated that the formation of $[BH_{4-x}F_x]^-$ causes a strong destabilization of $LiBH_4$, leading to a decomposition pathway forming diborane gas and solid decomposition products such as LiF and $Li_2B_{12}H_{12}$. This decomposition reaction pathway led the authors to conclude that this system does not hold promise of any practical usage in hydrogen desorption/absorption cycling [36]. Even if the conclusion of the authors can be considered correct, the studied system could be of interest in the SSE research field. In fact, it has been suggested that *closo*-borate anions (e.g., $B_{12}H_{12}^{2-}$) have lower reduction ability than BH_4^- and thus show higher electrochemical stability, in addition to a higher RT Li-ion conductivity [37].

Recently, Zhu et al. [36] reported that partial dehydrogenation of $LiBH_4$ results in the in-situ formation of highly conductive Li−B−H complexes, containing $LiBH_4$, $[Li_2B_{12}H_{11+1/n}]_n$ and LiH. A dramatic increase in Li-ion conductivity to 2.7×10^{-4} S cm^{-1} at 35 °C is observed, likely due to the presence of a highly conductive interface between $[Li_2B_{12}H_{11+1/n}]_n$ and $LiBH_4$ [38]. Although the exact phase is still under debate, these Li−B−H complexes are believed to contain *closo*-borates [39]. We expect that similar in-situ formed Li−B−H complexes can be derived from the destabilization of $LiBH_4$ caused by $LiBF_4$, which may exhibit superior Li-ion conducting performances.

In this work, we explore the impact of $LiBF_4$ incorporation on $LiBH_4$, especially looking into the ionic conductivity of in-situ formed Li-B-H complexes. The structural properties and ionic conductivity of the synthetized mixtures are analysed to investigate how the presence of BF_4^- in the mixtures affects the Li-B-H complex composition and structure, as well as the lithium-ion mobility.

2. Experimental Section

2.1. Solid-State Synthesis

Several $LiBH_4$-$LiBF_4$ and $LiBH_4$-$Li_2B_{12}H_{12}$ mixtures were prepared by physically mixing $LiBH_4$ (purity > 95%, Sigma-Aldrich, St. Louis, MO, USA) with either 20 mol% of $LiBF_4$ (purity > 98%, Sigma-Aldrich) or 25 mol% of anhydrous $Li_2B_{12}H_{12}$ (purity > 98%, Katchem, Prague, Czech Republic) in an agate mortar approximately 5 min. The physical mixtures were transferred into a stainless-steel reactor, which was placed in a stainless-steel high-pressure autoclave (Parr, 250 mL). After pressurizing the autoclave with 50 bar of H_2, the physical mixtures were heated to 150 °C or 280 °C (heating rate 2.5 °C min^{-1}) for 30 min. The samples were collected from the autoclave after the heat treatment and analysed further. An overview of all prepared samples is provided in Table S1. All storage and handling of the chemicals and prepared samples was carried out in an argon-filled glovebox (H_2O and O_2 < 0.1 ppm).

2.2. Structural Characterization

X-ray powder diffraction (XRD) analysis was performed with a Bruker-AXS D8 Advance X-ray diffractometer (Co Kα_1 = 1.78897 Å). The samples were placed in an airtight sample holder, preventing air and moisture exposure. Diffractograms were recorded at RT from 20° to 80° 2θ range.

Diffuse reflectance infrared Fourier transform spectroscopy (DRIFTS) measurements were performed on a Perkin-Elmer 2000 spectrometer equipped with an MCT detector. Using an airtight sample holder with KBr windows, samples were measured without any air or moisture exposure. Spectra were acquired from 900 cm^{-1} to 4500 cm^{-1} with a resolution of 4 cm^{-1}.

2.3. Electrochemical Impedance Spectroscopy

Electrochemical impedance spectroscopy (EIS) measurements were performed using a Princeton Applied Research Parstat 2273 connected to a custom-made measurement cell in a Büchi B-585 glass oven. Two stainless steel cylinders with Li foil (Sigma-Aldrich, purity 99.9%, 0.38 mm thick) were placed on one side and configured as electrodes. Using a standard 13 mm pellet press, an approximately 80–150 mg sample was pressed between the electrodes with a pressure of approximately 1.5 ton cm^{-2}. During a typical conductivity measurement, the measurement cell was incrementally heated to 130 °C (ΔT = 10 °C) and incrementally cooled to room temperature (ΔT = 20 °C). At each increment the temperature was allowed to equilibrate before an EIS measurement was performed using a 10 mV of amplitude and with frequencies from 1 MHz to 1 Hz.

2.4. Linear Sweep Voltammetry

Linear sweep voltammetry (LSV) was used to determine the oxidative stability of the $LiBH_4$-20% $LiBF_4$ sample. The sample was mixed with carbon black (CB, Ketjenblack EC600JD) in a weight ratio of 90:10 using an agate mortar. A pellet was obtained by pressing approximately 5 mg of electrolyte-carbon mixture and 50 mg of the electrolyte at 1.5 ton cm^{-2}. After compressing, a cell was formed with stainless-steel as the working electrode in contact with the electrolyte-carbon mixture and a lithium disk as the counter electrode in contact with the solid electrolyte. The linear sweep measurement was performed at 60 °C with a voltage range from 1.0 V to 5.0 V versus Li^+/Li at a scanning rate of 0.1 mVs^{-1}.

3. Results and Discussion

3.1. Structural Characterization and Conductivity of $LiBH_4$-$LiBF_4$ Mixtures

The impact of the addition of $LiBF_4$ on the crystal structure of the Li-B-H complexes has been determined using XRD. In Figure 1a, the diffractograms of a mixture consisting of 80 mol% of $LiBH_4$ and 20 mol% $LiBF_4$ prepared via solid-state reaction at 150 °C and 280 °C are shown. The XRD patterns of $LiBH_4$ and $LiBF_4$ are provided for comparison. In

the diffraction pattern of the $LiBH_4$-$LiBF_4$ mixture heated at 150 °C, the main diffraction peaks characteristic of both starting compounds are still observed. Additionally, two new peaks have appeared at 45 and 53 2θ°, that correspond to cubic (*Fm-3m*) LiF. This can be explained considering that the decomposition of $LiBH_4$ in the presence of $LiBF_4$ starts at 80 °C and LiF has been reported as a decomposition product [36]. During the reaction, hydrogen-fluorine exchange results in the formation of $LiBH_{4-x}F_x$ [36], which is not stable and decomposes to form LiF.

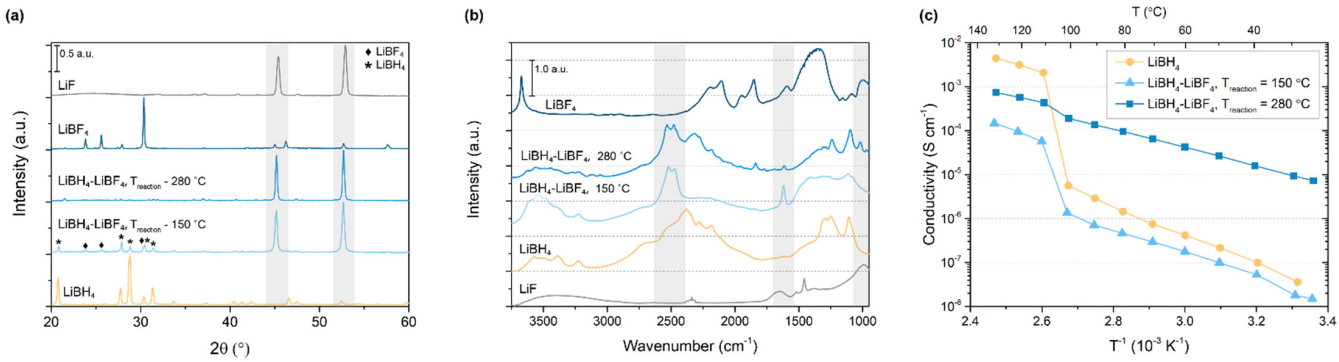

Figure 1. (**a**) X-ray powder diffraction patterns, (**b**) DRIFTS spectra and (**c**) Arrhenius conductivity plots of $LiBH_4$-$LiBF_4$ mixtures prepared at 150 °C and 280 °C. For comparison, $LiBH_4$, $LiBF_4$ and LiF are included in the XRD patterns; the spectra of $LiBH_4$, $LiBF_4$ and LiF are shown in the DRIFTS spectra and the ionic conductivity of pristine $LiBH_4$ is added to the Arrhenius plots. Relevant reflections are highlighted in grey.

Similarly, the diffraction pattern of the $LiBH_4$-$LiBF_4$ mixture prepared at 280 °C predominantly contains peaks related to LiF; however, in this case no clear diffraction peaks of the starting compounds can be identified. Thus, at a reaction temperature of 280 °C, the decomposition reaction proceeds further in agreement with results reported by Richter et al. [36] Note that with XRD only crystalline compounds can be identified. Therefore, it is not clear whether LiF is the only solid decomposition product or if an unidentified amorphous phase is formed as well. For example, Zhu et al. reported that highly conductive amorphous Li-B-H complexes can form during the $LiBH_4$ decomposition [38].

Because with the XRD analysis the presence of possible amorphous Li-B-H complexes could not be confirmed, the structural properties of the $LiBH_4$-$LiBF_4$ mixtures were further analysed using DRIFTS measurements. This technique is not limited to crystalline compounds, which means that it can be used to identify the composition of the crystalline and amorphous phases present in the $LiBH_4$-$LiBF_4$ mixtures. The DRIFTS absorbance spectra obtained for $LiBH_4$-$LiBF_4$ synthesized at 150 °C and 280 °C are shown in Figure 1b, as well as the spectra for pristine $LiBH_4$ and $LiBF_4$. Pristine $LiBH_4$ typically shows several characteristic absorption bands. The most predominant bands, corresponding to [BH_4^-] stretching vibrations, can be seen between 2000 and 2800 cm^{-1}. Other characteristic $LiBH_4$ vibrations can be seen between 1000 and 1300 cm^{-1} ([BH_4^-] bending) and 3200 and 3700 cm^{-1} ([OH] stretching from adsorbed moisture) [40–42]. Though less intense, these characteristic bands are seen in the spectra of both $LiBH_4$-$LiBF_4$ mixtures, indicating that $LiBH_4$ is still present in both mixed compounds, hence the starting compounds have not completely decomposed. Note that the bands related to $LiBH_4$ vibrations are especially pronounced in the DRIFTS spectrum of $LiBH_4$-$LiBF_4$ prepared at 280 °C, even though no peaks related to crystalline $LiBH_4$ were present in the diffractogram, suggesting that residual amorphous $LiBH_4$ is present in the compound.

Besides the $LiBH_4$ vibrations, multiple unidentified peaks are present in both $LiBH_4$-$LiBF_4$ spectra, specifically around 2500 cm^{-1} and at 1800 cm^{-1}. Surprisingly, none of these peaks is related to the presence of $LiBF_4$ or LiF (Figure 1b) [40,43]. Clearly, decomposition of the unstable $LiBH_{4-x}F_x$ complex does not only result in the formation of LiF, but also

in an unidentified amorphous compound. Similar to the Li-B-H complexes obtained during $LiBH_4$ decomposition described by Zhu et al., this unidentified compound could be beneficial for the overall conductivity of the $LiBH_4$-$LiBF_4$ compounds [38]. Therefore, the nature of this compound has been studied in more detail, which will be discussed later in this work.

The impact of the decomposition reaction on Li-ion conductivity in the prepared $LiBH_4$-$LiBF_4$ mixed compounds is determined using electrochemical impedance spectroscopy (EIS). The obtained Nyquist plots display single semicircles that could be analysed with a simple one-phase model, as is shown in Figure S1. Additionally, exemplary Bode plots corresponding to the data are shown in Figure S2. In this way, the resistance and corresponding conductivity are determined over a temperature range from room temperature to 130 °C. In Figure 1c and Figure S3, the temperature dependence of the ionic conductivity of the $LiBH_4$-$LiBF_4$ mixtures prepared at 150 °C and 280 °C is displayed using an Arrhenius plot. Comparison to the ionic conductivity of $LiBH_4$ shows that ion transport in the $LiBH_4$-$LiBF_4$ mixtures prepared at 280 °C has improved at temperatures lower than 100 °C, reaching 0.9×10^{-5} S cm^{-1} at 30 °C, which is three orders of magnitude higher than that of $LiBH_4$. In contrast, the mixture prepared with a lower reaction temperature exhibits a conductivity lower than that of $LiBH_4$ over the entire temperature range.

At temperatures above 110 °C, the same temperature-dependent Li-ion conductivity behaviour as $LiBH_4$ has been measured for the mixture treated at 150 °C, i.e., a drastic increase of the Li-ion conductivity. This behaviour indicates that the sample contains unreacted $LiBH_4$ that undergoes a phase transition from the orthorhombic to the hexagonal phase, increasing the Li-ion conductivity. These results agree with both the diffraction and IR data reported in Figure 1. The lower ion conductivity with respect to pure $LiBH_4$ can be explained considering that the sample also contains non-conductive phases, i.e., unreacted $LiBF_4$ and LiF. The $LiBH_4$-$LiBF_4$ mixture prepared at 280 °C also exhibits a conductivity enhancement above 110 °C related to the phase transition of $LiBH_4$, though it is not as pronounced. The conductivity above 110 °C is lower than that of pristine $LiBH_4$, which again can be attributed to the presence of non-conductive LiF.

The difference in conductivity between the mixtures prepared with different reaction temperature (see also Figure S4) indicates that the reaction temperature of the prepared $LiBH_4$-$LiBF_4$ system plays an important role. It is not likely that LiF predominantly contributes to the enhanced conductivity, as it does not exhibit high room temperature conductivity by itself, typically below 10^{-7} S cm^{-1} [44,45]. On the other hand, the incorporation of LiF could lead to the formation of a LiF-substituted $LiBH_4$ solid solution in which the hexagonal $LiBH_4$ phase is stabilized at lower temperatures. However, previous studies on halide substituted $LiBH_4$ demonstrated that the RT stability range of the hexagonal phase decreases with the anionic radius. In fact, it has been reported that h-$Li(BH_4)_{1-\alpha}(I)_\alpha$ solid solutions are stable at RT in the range of $0.18 \leq \alpha \leq 0.50$, [46,47] h-$Li(BH_4)_{1-\alpha}(Br)_\alpha$ in the range $0.3 \leq \alpha \leq 0.55$ [29], while Cl^- is not able to stabilize the high temperature phase at RT [46]. The ionic size of F^- is considerably smaller with respect to BH_4^- as well as to the other halides, i.e., $r(F^-)$ = 1.33 Å, $r(Cl^-)$ = 1.81 Å, $r(Br^-)$ = 1.96 Å, $r(I^-)$ = 2.20 Å and $r(BH_4^-)$ = 2.03 Å [48], which makes stabilization of the hexagonal phase at ambient temperature unlikely. This hypothesis is further confirmed by the absence of reflections related to hexagonal $LiBH_4$ in the $LiBH_4$-$LiBF_4$ diffraction patterns (Figure 1a). Consequently, it is not expected that the formation of LiF contributes to conductivity enhancement in the $LiBH_4$-$LiBF_4$ compound.

Nevertheless, it is clear that a highly conductive compound forms after the solid-state reaction occurring at 280 °C, during which hydrogen-fluoride substitution and subsequent decomposition of $LiBH_{4-x}F_x$ occur. Because an improved conductivity is only seen in this case, it seems that the decomposition reaction that results in the presence of amorphous $LiBH_4$ and the formation of the unidentified compound (only observed in DRIFTS) is of vital importance to the conductivity enhancement. Richter et al. established a decomposition

pathway of $LiBH_3F$ (Figure 2) that could explain the conductivity enhancement in the $LiBH_4$-$LiBF_4$ mixture [36].

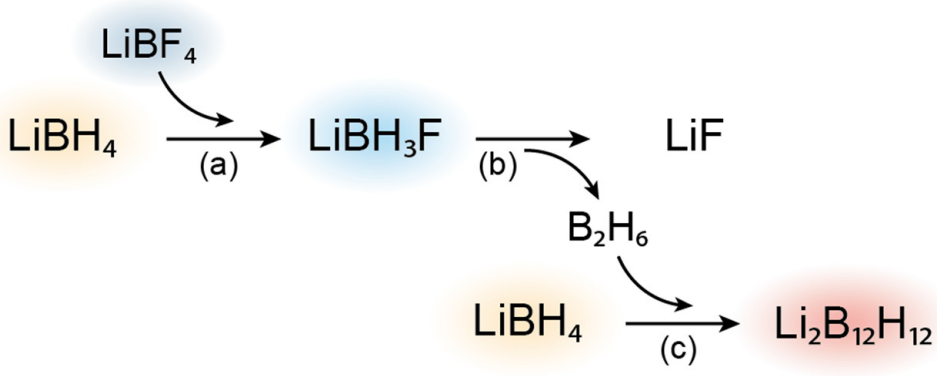

Figure 2. Reaction overview for $LiBH_4$-$LiBF_4$ solid solutions as proposed by Richter et al. [36]. (**a**) Hydrogen-fluorine exchange of $LiBF_4$ with $LiBH_4$ to form $LiBH_3F$. (**b**) Decomposition of the substituted material yielding LiF and B_2H_6. (**c**) Reaction of B_2H_6 with excess $LiBH_4$ forming $Li_2B_{12}H_{12}$. Reaction stoichiometry not taken in account in this overview.

Their analysis illustrates that the formation of $LiBH_3F$ from hydrogen-fluorine substitution does not solely result in the formation of LiF. The highly unstable $LiBH_3F$ compound decomposes to form both LiF and diborane (B_2H_6). Finally, diborane can react with an excess of $LiBH_4$ to form $Li_2B_{12}H_{12}$. Because the studied composition consists of 80 mol% of $LiBH_4$, it is possible for this final reaction (Figure 2c) to occur. This decomposition pathway can support our observations on the effect of hydrogen-fluorine exchange and decomposition of the $LiBH_4$-$LiBF_4$ mixtures together with the enhancement of the Li-ion conductivity.

3.2. *$LiBH_4$-$Li_2B_{12}H_{12}$ Composites*

To investigate if the high ionic conductivity is related to the formation of $Li_2B_{12}H_{12}$-like or $LiBH_4$-$Li_2B_{12}H_{12}$ composites during the decomposition reaction, mixtures of $LiBH_4$ with 10 to 75 mol% $Li_2B_{12}H_{12}$ (see Table S1) were prepared following the synthetic procedure used for the mixture $LiBH_4$-$LiBF_4$ synthetized at 280 °C. The composition based on 25 mol% $Li_2B_{12}H_{12}$ will be discussed below because it resembles the composition of the $LiBH_4$-$LiBF_4$ mixture. The DRIFTS and XRD spectra of the $LiBH_4$-25% $Li_2B_{12}H_{12}$ sample prepared are shown in Figure 3, together with those obtained from the $LiBH_4$-$LiBF_4$ system, while in Figure S5 the other $LiBH_4$-$Li_2B_{12}H_{12}$ samples are presented. In Figure 3a, the DRIFTS spectra of both $LiBH_4$-$LiBF_4$ and $LiBH_4$-$Li_2B_{12}H_{12}$ contain strong absorption bands at 2535 cm^{-1} and 2480 cm^{-1}. The previously unidentified peaks in the $LiBH_4$-$LiBF_4$ spectrum can thus be associated with the presence of $Li_2B_{12}H_{12}$, which displays characteristic [B-H] stretching vibrations exactly at these wavenumbers [49–51]. Other similarities in the DRIFTS spectra of $LiBH_4$-$LiBF_4$ and $LiBH_4$-$Li_2B_{12}H_{12}$ are also observed. The comparison reveals that, in addition to the pronounced bands around 2500 cm^{-1}, smaller peaks between 3700 and 3000 cm^{-1}, at 1835 cm^{-1} and at 1015 cm^{-1}, can also be explained by the presence of $Li_2B_{12}H_{12}$ [49–51]. Together with the XRD results discussed previously (Figure 1b), this illustrates that the prepared $LiBH_4$-$LiBF_4$ mixtures decompose to form crystalline LiF and likely amorphous *closo*-borate-related compounds with residual $LiBH_4$.

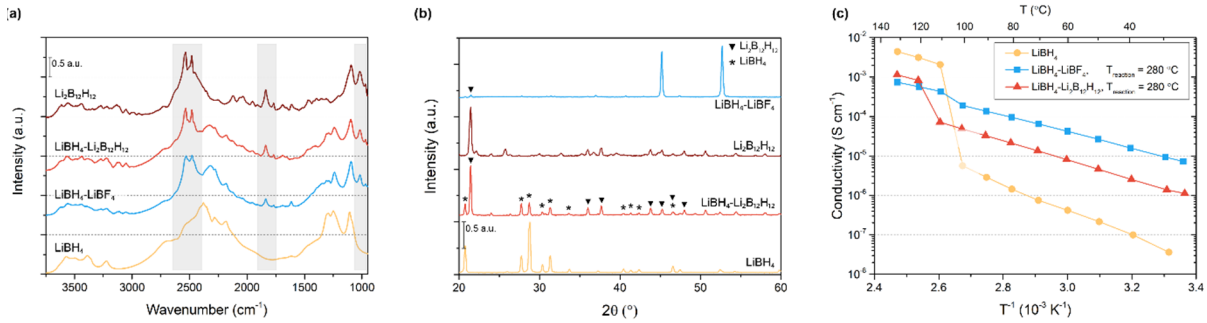

Figure 3. (**a**) DRIFTS spectra, (**b**) XRD diffraction patterns and (**c**) Arrhenius conductivity plots of $LiBH_4$-$LiBF_4$ and $LiBH_4$-$Li_2B_{12}H_{12}$ mixtures synthetized at 280 °C. In the DRIFTS and XRD graphs, $LiBH_4$ and $Li_2B_{12}H_{12}$ are included for comparison. In the DRIFTS, spectra peaks related to $Li_2B_{12}H_{12}$ vibrations are highlighted in grey.

This assertion is further investigated by comparing the XRD patterns of $LiBH_4$-$LiBF_4$ to that of $LiBH_4$-$Li_2B_{12}H_{12}$ shown in Figure 3b. Notably, the pattern collected for the $LiBH_4$-$Li_2B_{12}H_{12}$ contains characteristic diffraction peaks related to both starting compounds, which clearly demonstrates that both phases are still present and crystalline. This is different from the pattern of $LiBH_4$-$LiBF_4$, where, besides LiF, no other crystalline phase is detected. Note that a small peak indicative of $Li_2B_{12}H_{12}$ can be observed at 24 2θ° in the $LiBH_4$-$LiBF_4$ mixture pattern, strengthening the possibility that $Li_2B_{12}H_{12}$ has formed. However, in general it seems that the reaction between $LiBF_4$ and $LiBH_4$ leads to partial decomposition forming crystalline LiF and amorphous $Li_2B_{12}H_{12}$. Several studies have shown that the incorporation of $Li_2B_{12}H_{12}$ in the $LiBH_4$ matrix could lead to enhanced lithium-ion mobility [38,52–54]. Similar to the Li-B-H compound proposed by Zhu et al. [38], after reaction the $LiBH_4$-$LiBF_4$ mixture consists of residual $LiBH_4$ in contact with LiF and amorphous $Li_2B_{12}H_{12}$. Accordingly, the conductivity enhancement could originate from the in-situ formation of $Li_2B_{12}H_{12}$.

To further investigate this hypothesis, electrochemical impedance spectroscopy was used to determine the conductivity of $LiBH_4$-$Li_2B_{12}H_{12}$. Interestingly, in Figure 3c and Figure S6, it can be seen that the conductivity of $LiBH_4$-$Li_2B_{12}H_{12}$ (0.5×10^{-6} S cm^{-1} at RT) is improved compared to both pristine $LiBH_4$ and $Li_2B_{12}H_{12}$ (2.5×10^{-8} S cm^{-1} at RT) [55]. The improvement in ionic conductivity can be attributed again to a partial $LiBH_4$ decomposition, to form some amorphous $Li_2B_{12}H_{12}$ or $[Li_2B_{12}H_{11+1/n}]_n$ and undecomposed $LiBH_4$ (see also next paragraph). Consequently, the improved cation mobility observed in the $LiBH_4$-$LiBF_4$ mixture prepared at 280 °C can be attributed to the formation of $Li_2B_{12}H_{12}$ and its interaction with residual $LiBH_4$, while the presence of LiF likely has a minor or no impact.

Table 1 shows the values of the activation energies (E_a) obtained by a linear fit of the Arrhenius plot. The E_a of the orthorhombic $LiBH_4$ is in good agreement with the calculated average value using all values reported in the literature by Gulino et al. [56], i.e., 0.75 ± 0.07 eV. The E_a obtained for the mixtures $LiBH_4$-$LiBF_4$ and $LiBH_4$-$Li_2B_{12}H_{12}$ are lower compared to that of pure $LiBH_4$, indicating a more facile conduction mechanism, in agreement with the higher Li-ion conductivity. In addition, these values are in agreement with the data reported by Zhu et al. [38], e.g., 0.43 eV and 0.44 eV for the samples containing amorphous $Li_2B_{12}H_{12}$ or $[Li_2B_{12}H_{11+1/n}]_n$, further indicating that the highly conductivity phase formed during reaction with $LiBF_4$ could be amorphous $Li_2B_{12}H_{12}$ or a related compound. It is also good to note that the oxidative stability of 4.0 V determined for the $LiBH_4$-$LiBF_4$ mixture (Figure S7) is similar to the value reported for other *closo*-borate-related compounds [13,38,57].

Table 1. Activation energies (eV) calculated from a linear plot of ln(σT) and 1000/T of the EIS data reported in Figure 3c. The standard deviation is based on the 99% confidence interval of the linear fit.

Sample	E_a (eV)	Pre-Exponential Factor
LiBH4 (orthorhombic)	0.68 (±0.05)	15 (±2)
LiBH4-LiBF4 (280 °C)	0.44 (±0.01)	11.1 (±0.3)
LiBH4-Li2B12H12 (280 °C)	0.41 (±0.01)	11.8 (±0.4)

3.3. Alternative Decomposition Pathway

Although it seems clear that the formation of a $Li_2B_{12}H_{12}$-like compound is responsible for the enhancement in ionic conductivity for $LiBH_4$-$LiBF_4$, this could not explain the behaviour of the system completely. Surprisingly, comparison of the respective conductivities of $LiBH_4$-$Li_2B_{12}H_{12}$ and $LiBH_4$-$LiBF_4$ mixtures (Figure 3c) illustrates that the latter has the highest conductivity. If the conductivity enhancement is solely related to the formation of $Li_2B_{12}H_{12}$, this would not be the case. However, as our structural analysis did not yield any other compounds or phases, the unidentified conductive phase is likely very similar to amorphous $Li_2B_{12}H_{12}$.

Interestingly, it has been proposed that the combination of different *closo*-borate complex anions could lead to improved ion transport in metal hydride-based ion conductors [38,54,58,59]. Toyama et al. prepared complex hydrides containing three *closo*-borate-type anions, e.g., $[B_{12}H_{12}]^{2-}$, $[B_{11}H_{11}]^{2-}$ and $[B_{10}H_{10}]^{2-}$, from $LiBH_4$ and $B_{10}H_{14}$ as the starting materials [54]. They observed that with increasing amount of $[B_{11}H_{11}]^{2-}$ and $[B_{10}H_{10}]^{2-}$, ionic conductivity improves. Remarkably, under the reaction conditions used during our synthesis, pyrolysis of B_2H_6 to $B_{10}H_{14}$ can occur [60,61]. The in-situ generated $B_{10}H_{14}$ can then react with $LiBH_4$ to form several *closo*-borate anions, similar to the synthesis performed by Toyama et al. [54] The reaction scheme discussed here is presented in Figure 4.

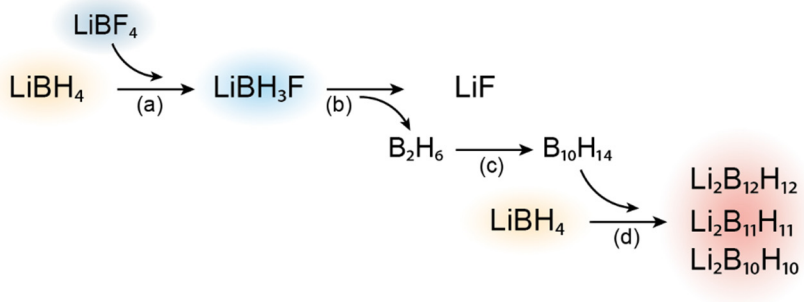

Figure 4. Reaction scheme proposed for the synthesis of $LiBH_4$-$LiBF_4$ solid solutions constituted of multiple *closo*-borate phases. (**a**) Reaction between $LiBF_4$ and $LiBH_4$ yielding unstable $LiBH_3F$ followed by (**b**) decomposition to form LiF and B_2H_6. (**c**) Pyrolysis of B_2H_6 generating $B_{10}H_{14}$ in-situ. (**d**) Reaction of $B_{10}H_{14}$ with $LiBH_4$ forming several lithium *closo*-borates. Reaction stoichiometry not taken in account in this overview.

The conductivity enhancement achieved in decomposed $LiBH_4$ in the presence of $LiBF_4$ that forms multiple *closo*-borate phases would be higher than expected for a mixture consisting solely of $LiBH_4$ and $Li_2B_{12}H_{12}$. Consequently, the reaction process described in Figure 4 provides a possible explanation for an increased conductivity in $LiBH_4$-$LiBF_4$ compared to $LiBH_4$-$Li_2B_{12}H_{12}$ through the introduction of different lithium *closo*-borate compounds. A detailed investigation of this hypothesis will require solid-state ^{11}B-MAS-NMR measurements, which is the subject of an ongoing study.

Another explanation for the enhanced conductivity could be the formation of highly conductive interfaces between the amorphous $LiBH_4$-$Li_2B_{12}H_{12}$ solid solution and the in-situ formed nanocrystalline LiF particles. The melting of the undecomposed $LiBH_4$

will likely lead to strong interface interactions with LiF and $Li_2B_{12}H_{12}$, thereby enhancing the ionic conductivity of the composite. Recent studies by Yan and Zhao reported on similar systems in which $LiBH_4$ xNH_3 was stabilized in an amorphous (molten-like) state on (inert) Li_2O nanoparticles that were formed in-situ via a decomposition pathway [62,63]. Even in compounds with a high weight percentage (78 wt%) of the non-conducting metal oxide, a high room temperature conductivity has been obtained. Likewise, in our case, the amorphous $LiBH_4$-$Li_2B_{12}H_{12}$ phase could benefit from the presence of LiF particles, for example by stabilizing the amorphous form or even by beneficial interface interactions, thereby forming a conductive space-charge layer.

4. Conclusions

In conclusion, the impact of $LiBF_4$ addition on the ionic transport in $LiBH_4$ was explored by correlating the physical properties and ionic conductivity of $LiBH_4$-$LiBF_4$ mixtures. After synthesis at 280 °C, the $LiBH_4$-$LiBF_4$ sample contains LiF and amorphous lithium *closo*-borate, such as $Li_2B_{12}H_{12}$. The presence of this phase is in line with the fact that partial substitution of the BH_4 anion in $LiBH_4$ with BF_4 anion yields unstable $LiBH_3F$, which decomposes into LiF and B_2H_6. The latter may react further to form $B_{10}H_{14}$, which in turn leads to the formation of $[B_{12}H_{12}]^{2-}$, $[B_{11}H_{11}]^{2-}$ and $[B_{10}H_{10}]^{2-}$ complex anions by reacting with excess $LiBH_4$.

Interestingly, a conductivity enhancement of over two orders of magnitude (to 0.9×10^{-5} S cm^{-1} at 30 °C) is achieved for the $LiBH_4$-$LiBF_4$ mixture reacted at 280 °C. The formation of LiF does not seem to lead to any improvement in conductivity, while the presence of solely $Li_2B_{12}H_{12}$ leads to a minor enhancement. Thus, the improved lithium-ion mobility in $LiBH_4$ through decomposition reaction with $LiBF_4$ may be attributed to the formation of a lithium *closo*-borate-like phase, i.e., amorphous $Li_2B_{12}H_{12}$ or $[Li_2B_{12}H_{11+1/n}]_n$. The insights provided in this work highlight the versatility of $LiBH_4$ as a promising solid-state electrolyte, considering that several different strategies can be exploited to increase the ionic conductivity of the compound. Our work demonstrates that decomposition reactions is a promising approach to enhancing ionic conductivity in $LiBH_4$. This approach might be applicable to other complex hydrides and other classes of inorganic solid electrolytes.

Supplementary Materials: The following supporting information can be downloaded at: https://www.mdpi.com/article/10.3390/molecules27072187/s1, Table S1: Overview of the sample compositions, Figure S1: Nyquist plots of two exemplary samples, Figure S2: Bode plots of two exemplary samples, Figures S3 and S4: conductivity data of $LiBH_4$-$LiBF_4$ samples prepared with different compositions and under varying synthesis conditions, Figures S5 and S6: characterization of $LiBH_4$-$Li_2B_{12}H_{12}$ samples with varying composition and Figure S7: a linear sweep voltammogram of $LiBH_4$-$LiBF_4$.

Author Contributions: Conceptualization, P.N. and L.M.d.K.; formal analysis, P.N., L.M.d.K. and D.B.; data curation, L.M.d.K., P.N. and D.B.; writing—review and editing, P.N., L.M.d.K., V.G. and D.B.; project administration, P.N. All authors have read and agreed to the published version of the manuscript.

Funding: Dutch Research Council (NWO) Materials for sustainability Mat4Sus (739.017.009) grant.

Institutional Review Board Statement: Not appliable.

Informed Consent Statement: Not appliable.

Data Availability Statement: The data presented in this study are available in supplementary material.

Acknowledgments: The authors greatly appreciate the fruitful discussions with Petra de Jongh, Jan Willem de Rijk is acknowledged for technical support.

Conflicts of Interest: The authors declare no conflict of interest.

References

1. Lach, J.; Wróbel, K.; Wróbel, J.; Czerwiński, A. Applications of carbon in rechargeable electrochemical power sources: A review. *Energies* **2021**, *14*, 2649. [CrossRef]
2. Li, C.; Wang, Z.Y.; He, Z.J.; Li, Y.J.; Mao, J.; Dai, K.H.; Yan, C.; Zheng, J.C. An advance review of solid-state battery: Challenges, progress and prospects. *Sustain. Mater. Technol.* **2021**, *29*, e00297. [CrossRef]
3. Tarascon, J.M.; Armand, M. Issues and challenges facing rechargeable lithium batteries. *Nature* **2001**, *414*, 359–367. [CrossRef] [PubMed]
4. Janek, J.; Zeier, W.G. A solid future for battery development. *Nat. Energy* **2016**, *1*, 16141. [CrossRef]
5. Manthiram, A.; Yu, X.; Wang, S. Lithium battery chemistries enabled by solid-state electrolytes. *Nat. Rev. Mater.* **2017**, *2*, 16103. [CrossRef]
6. Thangadurai, V.; Narayanan, S.; Pinzaru, D. Garnet-type solid-state fast Li ion conductors for Li batteries: Critical review. *Chem. Soc. Rev.* **2014**, *43*, 4714–4727. [CrossRef]
7. Subramanian, K.; Alexander, G.V.; Karthik, K.; Patra, S.; Indu, M.S.; Sreejith, O.V.; Viswanathan, R.; Narayanasamy, J.; Murugan, R. A brief review of recent advances in garnet structured solid electrolyte based lithium metal batteries. *J. Energy Storage* **2021**, *33*, 102157. [CrossRef]
8. Thangadurai, V.; Weppner, W. Recent progress in solid oxide and lithium ion conducting electrolytes research. *Ionics* **2006**, *12*, 81–92. [CrossRef]
9. Itoh, M.; Inaguma, Y.; Jung, W.H.; Chen, L.; Nakamura, T. High lithium ion conductivity in the perovskite-type compounds $Ln_{12}Li_{12}TiO_3$ (Ln=La,Pr,Nd,Sm). *Solid State Ion.* **1994**, *70–71*, 203–207. [CrossRef]
10. Seino, Y.; Ota, T.; Takada, K.; Hayashi, A.; Tatsumisago, M. A sulphide lithium super ion conductor is superior to liquid ion conductors for use in rechargeable batteries. *Energy Environ. Sci.* **2014**, *7*, 627–631. [CrossRef]
11. Rangasamy, E.; Liu, Z.; Gobet, M.; Pilar, K.; Sahu, G.; Zhou, W.; Wu, H.; Greenbaum, S.; Liang, C. An iodide-based $Li_7P_2S_8I$ superionic conductor. *J. Am. Chem. Soc.* **2015**, *137*, 1384–1387. [CrossRef] [PubMed]
12. Matsuo, M.; Nakamori, Y.; Orimo, S.I.; Maekawa, H.; Takamura, H. Lithium superionic conduction in lithium borohydride accompanied by structural transition. *Appl. Phys. Lett.* **2007**, *91*, 2–5. [CrossRef]
13. Lu, Z.; Ciucci, F. Metal Borohydrides as Electrolytes for Solid-State Li, Na, Mg, and Ca Batteries: A First-Principles Study. *Chem. Mater.* **2017**, *29*, 9308–9319. [CrossRef]
14. Asakura, R.; Duchêne, L.; Kühnel, R.S.; Remhof, A.; Hagemann, H.; Battaglia, C. Electrochemical Oxidative Stability of Hydroborate-Based Solid-State Electrolytes. *ACS Appl. Energy Mater.* **2019**, *2*, 6924–6930. [CrossRef]
15. Kisu, K.; Kim, S.; Oguchi, H.; Toyama, N.; Orimo, S.I. Interfacial stability between $LiBH_4$-based complex hydride solid electrolytes and Li metal anode for all-solid-state Li batteries. *J. Power Sour.* **2019**, *436*, 226821. [CrossRef]
16. Duchêne, L.; Remhof, A.; Hagemann, H.; Battaglia, C. Status and prospects of hydroborate electrolytes for all-solid-state batteries. *Energy Storage Mater.* **2020**, *25*, 782–794. [CrossRef]
17. Verdal, N.; Udovic, T.J.; Stavila, V.; Tang, W.S.; Rush, J.J.; Skripov, A.V. Anion reorientations in the superionic conducting phase of $Na_2B_{12}H_{12}$. *J. Phys. Chem. C* **2014**, *118*, 17483–17489. [CrossRef]
18. Tang, W.S.; Matsuo, M.; Wu, H.; Stavila, V.; Zhou, W.; Talin, A.A.; Soloninin, A.V.; Skoryunov, R.V.; Babanova, O.A.; Skripov, A.V.; et al. Liquid-Like Ionic Conduction in Solid Lithium and Sodium Monocarba-closo-Decaborates Near or at Room Temperature. *Adv. Energy Mater.* **2016**, *6*, 1502237. [CrossRef]
19. Gulino, V.; Brighi, M.; Murgia, F.; Ngene, P.; De Jongh, P.; Černý, R.; Baricco, M. Room temperature Solid-State Lithium-ion Battery using LiBH4-MgO composite Electrolyte. *ACS Appl. Energy Mater.* **2021**, *4*, 1228–1236. [CrossRef]
20. Zettl, R.; De Kort, L.; Gombotz, M.; Wilkening, H.M.; De Jongh, P.E.; Ngene, P. Combined Effects of Anion Substitution and Nanoconfinement on the Ionic Conductivity of Li-Based Complex Hydrides. *J. Phys. Chem. C* **2020**, *124*, 2806–2816. [CrossRef]
21. De Kort, L.M.; Harmel, J.; De Jongh, P.E.; Ngene, P. The effect of nanoscaffold porosity and surface chemistry on the Li-ion conductivity of LiBH4-LiNH2/metal oxide nanocomposites. *J. Mater. Chem. A* **2020**, *8*, 20687–20697. [CrossRef]
22. De Kort, L.M.; Gulino, V.; de Jongh, P.E.; Ngene, P. Ionic conductivity in complex metal hydride-based nanocomposite materials: The impact of nanostructuring and nanocomposite formation. *J. Alloys Compd.* **2021**, *901*, 163474. [CrossRef]
23. Oguchi, H.; Matsuo, M.; Hummelshøj, J.S.; Vegge, T.; Nørskov, J.K.; Sato, T.; Miura, Y.; Takamura, H.; Maekawa, H.; Orimo, S. Experimental and computational studies on structural transitions in the LiBH4-LiI pseudobinary system. *Appl. Phys. Lett.* **2009**, *94*, 2–5. [CrossRef]
24. Matsuo, M.; Takamura, H.; Maekawa, H.; Li, H.-W.; Orimo, S. Stabilization of lithium superionic conduction phase and enhancement of conductivity of LiBH4 by LiCl addition. *Appl. Phys. Lett.* **2009**, *94*, 084103. [CrossRef]
25. Maekawa, H.; Matsuo, M.; Takamura, H.; Ando, M.; Noda, Y. Halide-Stabilized $LiBH_4$, a Room-Temperature Lithium Fast-Ion Conductor. *J. Am. Chem. Soc.* **2009**, *131*, 894–895.
26. Rude, L.H.; Groppo, E.; Arnbjerg, L.M.; Ravnsbaek, D.B.; Malmkjaer, R.A.; Filinchuk, Y.; Baricco, M.; Besenbacher, F.; Jensen, T.R. Iodide substitution in lithium borohydride, $LiBH_4$-LiI. *J. Alloys Compd.* **2011**, *509*, 8299–8305. [CrossRef]
27. Matsuo, M.; Remhof, A.; Martelli, P.; Caputo, R.; Ernst, M.; Miura, Y.; Sato, T.; Oguchi, H.; Maekawa, H.; Takamura, H. Complex hydrides with $(BH_4)^-$ and $(NH_2)^-$ anions as new lithium fast-ion conductors. *J. Am. Chem. Soc.* **2009**, *131*, 16389–16391. [CrossRef]
28. Yan, Y.; Kühnel, R.S.; Remhof, A.; Duchêne, L.; Reyes, E.C.; Rentsch, D.; Łodziana, Z.; Battaglia, C. A Lithium Amide-Borohydride Solid-State Electrolyte with Lithium-Ion Conductivities Comparable to Liquid Electrolytes. *Adv. Energy Mater.* **2017**, *7*, 1700294. [CrossRef]

29. Gulino, V.; Dematteis, E.M.; Corno, M.; Palumbo, M.; Baricco, M. Theoretical and Experimental Studies of $LiBH_4$–LiBr Phase Diagram. *ACS Appl. Energy Mater.* **2021**, *4*, 7327–7337.
30. Gulino, V.; Brighi, M.; Dematteis, E.M.; Murgia, F.; Nervi, C.; Cerny, R.; Baricco, M. Phase Stability and Fast Ion Conductivity in the Hexagonal LiBH4–LiBr–LiCl Solid Solution. *Chem. Mater.* **2019**, *31*, 5133–5144. [CrossRef]
31. Rude, L.H.; Filsø, U.; D'Anna, V.; Spyratou, A.; Richter, B.; Hino, S.; Zavorotynska, O.; Baricco, M.; Sørby, M.H.; Hauback, B.C. Hydrogen-fluorine exchange in NaBH4-NaBF4. *Phys. Chem. Chem. Phys.* **2013**, *15*, 18185–18194. [CrossRef] [PubMed]
32. Yin, L.; Wang, P.; Fang, Z.; Cheng, H. Thermodynamically tuning LiBH4 by fluorine anion doping for hydrogen storage: A density functional study. *Chem. Phys. Lett.* **2008**, *450*, 318–321. [CrossRef]
33. Corno, M.; Pinatel, E.; Ugliengo, P.; Baricco, M. A computational study on the effect of fluorine substitution in $LiBH_4$. *J. Alloy. Compd.* **2011**, *509*, S679–S683. [CrossRef]
34. Heyn, R.H.; Saldan, I.; Sørby, M.H.; Frommen, C.; Arstad, B.; Bougza, A.M.; Fjellvåg, H.; Hauback, B.C. Structural and spectroscopic characterization of potassium fluoroborohydrides. *Phys. Chem. Chem. Phys.* **2013**, *15*, 11226–11230. [CrossRef]
35. Saldin, V.I.; Sukhovey, V.V.; Savchenko, N.N.; Slobodyuk, A.B.; Ignatieva, L.N. Thermal studies of sodium tetrahydroborate–potassium tetrafluoroborate mixtures. *Russ. J. Inorg. Chem.* **2016**, *61*, 630–637. [CrossRef]
36. Richter, B.; Ravnsbæk, D.B.; Sharma, M.; Spyratou, A.; Hagemann, H.; Jensen, T.R. Fluoride substitution in LiBH4; Destabilization and decomposition. *Phys. Chem. Chem. Phys.* **2017**, *19*, 30157–30165. [CrossRef]
37. Brighi, M.; Murgia, F.; Černý, R. Closo-Hydroborate Sodium Salts as an Emerging Class of Room-Temperature Solid Electrolytes. *Cell Rep. Phys. Sci.* **2020**, *1*, 100217. [CrossRef]
38. Zhu, M.; Pang, Y.; Lu, F.; Shi, X.; Yang, J.; Zheng, S. In Situ Formed Li-B-H Complex with High Li-Ion Conductivity as a Potential Solid Electrolyte for Li Batteries. *ACS Appl. Mater. Interfaces* **2019**, *11*, 14136–14141. [CrossRef]
39. Ohba, N.; Miwa, K.; Aoki, M.; Noritake, T.; Towata, S.I.; Nakamori, Y.; Orimo, S.I.; Züttel, A. First-principles study on the stability of intermediate compounds of LiBH4. *Phys. Rev. B* **2006**, *74*, 075110. [CrossRef]
40. Zavorotynska, O.; Corno, M.; Damin, A.; Spoto, G.; Ugliengo, P.; Baricco, M. Vibrational properties of MBH4 and MBF4 crystals (M = Li, Na, K): A combined DFT, infrared, and Raman study. *J. Phys. Chem. C* **2011**, *115*, 18890–18900. [CrossRef]
41. D'Anna, V.; Spyratou, A.; Sharma, M.; Hagemann, H. FT-IR spectra of inorganic borohydrides. *Spectrochim. Acta Part A Mol. Biomol. Spectrosc.* **2014**, *128*, 902–906. [CrossRef] [PubMed]
42. Filinchuk, Y.; Hagemann, H. Structure and properties of $NaBH_4 \cdot 2H_2O$ and $NaBH_4$. *Eur. J. Inorg. Chem.* **2008**, *112*, 3127–3133. [CrossRef]
43. Raman, C.V. The vibration spectrum of lithium fluoride and the evaluation of its specific heat. *Proc. Indian Acad. Sci. Sect. A* **1962**, *55*, 131–152. [CrossRef]
44. Breuer, S.; Pregartner, V.; Lunghammer, S.; Wilkening, H.M.R. Dispersed Solid Conductors: Fast Interfacial Li-Ion Dynamics in Nanostructured LiF and LiF γ-Al_2O_3 Composites. *J. Phys. Chem. C* **2019**, *123*, 5222–5230. [CrossRef]
45. Li, C.; Gu, L.; Maier, J. Enhancement of the Li conductivity in LiF by introducing glass/crystal interfaces. *Adv. Funct. Mater.* **2012**, *22*, 1145–1149. [CrossRef]
46. Miyazaki, R.; Karahashi, T.; Kumatani, N.; Noda, Y.; Ando, M.; Takamura, H.; Matsuo, M.; Orimo, S.I.; Maekawa, H. Room temperature lithium fast-ion conduction and phase relationship of LiI stabilized LiBH4. *Solid State Ion.* **2011**, *192*, 143–147. [CrossRef]
47. Sveinbjörnsson, D.; Myrdal, J.S.; Blanchard, D.; Bentzen, J.J.; Hirata, T.; Mogensen, M.B.; Norby, P.; Orimo, S.I.; Vegge, T. Effect of Heat Treatment on the Lithium Ion Conduction of the LiBH4–LiI Solid Solution. *J. Phys. Chem. C* **2013**, *117*, 3249–3257. [CrossRef]
48. Shannon, R.D. Revised effective ionic radii and systematic studies of interatomic distances in halides and chalcogenides. *Acta Crystallogr. Sect. A* **1976**, *32*, 751–767. [CrossRef]
49. Muetterties, E.L.; Merrifield, R.E.; Miller, H.C.; Knoth, W.H.; Downing, J.R. Chemistry of Boranes. III. 1 The Infrared and Raman Spectra of B 12 H 12-and Related Anions. *J. Am. Chem. Soc.* **1962**, *84*, 2506–2508. [CrossRef]
50. Sharma, M.; Sethio, D.; D'Anna, V.; Hagemann, H. Theoretical study of B12Hn F (12-N)2-. *Int. J. Hydrogen Energy* **2015**, *40*, 12721–12726. [CrossRef]
51. Jensen, S.R.; Paskevicius, M.; Hansen, B.R.; Jakobsen, A.S.; Møller, K.T.; White, J.L.; Allendorf, M.D.; Stavila, V.; Skibsted, J.; Jensen, T.R. Hydrogenation properties of lithium and sodium hydride- closo -borate, [B10H10]2- and [B12H12]2-, composites. *Phys. Chem. Chem. Phys.* **2018**, *20*, 16266–16275. [CrossRef] [PubMed]
52. Sadikin, Y.; Brighi, M.; Schouwink, P.; Černý, R. Superionic Conduction of Sodium and Lithium in Anion-Mixed Hydroborates $Na_3BH_4B_{12}H_{12}$ and $(Li0.7Na_{0.3})_3BH_4B_{12}H_{12}$. *Adv. Energy Mater.* **2015**, *5*, 1501016. [CrossRef]
53. Sadikin, Y.; Skoryunov, R.V.; Babanova, O.A.; Soloninin, A.V.; Lodziana, Z.; Brighi, M.; Skripov, A.V.; Cerny, R. Anion Disorder in $K_3BH_4B_{12}H_{12}$ and Its Effect on Cation Mobility. *J. Phys. Chem. C* **2017**, *121*, 5503–5514. [CrossRef]
54. Toyama, N.; Kim, S.; Oguchi, H.; Sato, T.; Takagi, S.; Tazawa, M.; Nogami, G.; Orimo, S.I. Lithium ion conductivity of complex hydrides incorporating multiple closo-type complex anions. *J. Energy Chem.* **2019**, *38*, 84–87. [CrossRef]
55. Friedrichs, O.; Remhof, A.; Hwang, S.-J.; Züttel, A. Role of $Li_2B_{12}H_{12}$ for the Formation and Decomposition of LiBH4. *Chem. Mater.* **2010**, *22*, 3265–3268. [CrossRef]
56. Gulino, V.; Wolczyk, A.; Golov, A.A.; Eremin, R.A.; Palumbo, M.; Nervi, C.; Blatov, V.A.; Proserpio, D.M.; Baricco, M. Combined DFT and geometrical–topological analysis of Li-ion conductivity in complex hydrides. *Inorg. Chem. Front.* **2020**, *7*, 3115–3125. [CrossRef]

57. Asakura, R.; Reber, D.; Duchêne, L.; Payandeh, S.; Remhof, A.; Hagemann, H.; Battaglia, C. 4 V Room-Temperature All-Solid-State Sodium Battery Enabled By a Passivating Cathode/Hydroborate Solid Electrolyte Interface. *Energy Environ. Sci.* **2020**, *13*, 5048–5058. [CrossRef]
58. Yoshida, K.; Sato, T.; Unemoto, A.; Matsuo, M.; Ikeshoji, T.; Udovic, T.J.; Orimo, S.I. Fast sodium ionic conduction in Na2B10H10-Na2B12H12 pseudo-binary complex hydride and application to a bulk-type all-solid-state battery. *Appl. Phys. Lett.* **2017**, *110*, 103901. [CrossRef]
59. Duchêne, L.; Kühnel, R.S.; Rentsch, D.; Remhof, A.; Hagemann, H.; Battaglia, C. A highly stable sodium solid-state electrolyte based on a dodeca/deca-borate equimolar mixture. *Chem. Commun.* **2017**, *53*, 4195–4198. [CrossRef]
60. Polak, R.J.; Obenland, C. Pyrolysis of diborane. *Ind. Eng. Chem. Prod. Res. Dev.* **1964**, *3*, 234–238.
61. Dobson, J.; Maruca, R.; Schaeffer, R. Studies of Boranes. XXX. Reaction of Pentaborane (9) with Diborane (6). Isolation of Several New Boron Hydrides. *Inorg. Chem.* **1970**, *9*, 2161–2166. [CrossRef]
62. Zhao, W.; Zhang, R.; Li, H.; Zhang, Y.; Wang, Y.; Wu, C.; Yan, Y.; Chen, Y. Li-Ion Conductivity Enhancement of $LiBH_4 \cdot xNH_3$ with in Situ Formed Li_2O Nanoparticles. *ACS Appl. Mater. Interfaces* **2021**, *13*, 31635–31641. [CrossRef] [PubMed]
63. Yan, Y.; Grinderslev, J.B.; Lee, Y.S.; Jørgensen, M.; Cho, Y.W.; Černý, R.; Jensen, T.R. Ammonia-assisted fast Li-ion conductivity in a new hemiammine lithium borohydride, $LiBH_4 \cdot 1/2NH_3$. *Chem. Commun.* **2020**, *56*, 3971–3974. [CrossRef] [PubMed]